Developmental Cell *10*, 187–197, February, 2006 ©2006 Elsevier Inc. DOI 10.1016/j.devcel.2005.12.013

Genetic Elimination of Suppressor of Fused Reveals an Essential Repressor Function in the Mammalian Hedgehog Signaling Pathway

Jessica Svärd,[1,4] Karin Heby Henricson,[1,4] Madelen Persson-Lek,[2] Björn Rozell,[3] Matthias Lauth,[1] Åsa Bergström,[1] Johan Ericson,[2] Rune Toftgård,[1,*] and Stephan Teglund[1,*]

[1] Department of Biosciences at Novum
Karolinska Institutet
SE-141 57 Huddinge
Sweden

[2] Department of Cell and Molecular Biology
Karolinska Institutet
SE-171 77 Stockholm
Sweden

[3] Department of Laboratory Medicine
Karolinska University Hospital
Karolinska Institutet
SE-141 86 Huddinge
Sweden

Summary

The Hedgehog (Hh) pathway plays important roles during embryogenesis and carcinogenesis. Here, we show that ablation of the mouse Suppressor of fused (*Sufu*), an intracellular pathway component, leads to embryonic lethality at ~E9.5 with cephalic and neural tube defects. Fibroblasts derived from *Sufu*$^{-/-}$ embryos showed high Gli-mediated Hh pathway activity that could not be modulated at the level of Smoothened and could only partially be blocked by PKA activation. Despite the robust constitutive pathway activation in the *Sufu*$^{-/-}$ fibroblasts, the GLI1 steady-state localization remained largely cytoplasmic, implying the presence of an effective nuclear export mechanism. *Sufu*$^{+/-}$ mice develop a skin phenotype with basaloid changes and jaw keratocysts, characteristic features of Gorlin syndrome, a human genetic disease linked to enhanced Hh signaling. Our data demonstrate that, in striking contrast to *Drosophila*, in mammals, Sufu has a central role, and its loss of function leads to potent ligand-independent activation of the Hh pathway.

Introduction

The important roles that the Hedgehog (Hh) signaling pathway plays in embryonic development and tumorigenesis are well established (Hooper and Scott, 2005; Ingham and McMahon, 2001; Lum and Beachy, 2004). The core components of the pathway have been identified in most invertebrate and vertebrate animals studied and therefore have been viewed as an evolutionary well-conserved pathway. Signal transduction is initiated by binding of the extracellular Hh ligands to the 12-span transmembrane receptor Patched (Ptch), relieving the repressive effects that Ptch normally exerts upon the 7-span transmembrane protein Smoothened (Smo) (Ingham and McMahon, 2001). Signal transmission from Smo eventually leads to changes in the activity of the Ci/Gli transcription factors that ultimately decide the outcome of the Hh signal. In the pathway, downstream of Smo, a number of components are present that integrate the signal from Smo and regulate the status of Ci/Gli. Initially identified in *Drosophila*, these include the serine-threonine kinase Fused (Fu), Suppressor of fused (Sufu), and the microtubule binding kinesin-like molecule Costal 2 (Cos2). Sufu is a negative regulator of Hh signaling with a proposed role in nuclear-cytoplasmic shuttling of the Ci/Gli transcription factors (Kogerman et al., 1999). There appear to be two domains in Sufu, one in the NH_2 terminus and one in the COOH terminus, that are important for interacting with and regulating Ci/Gli (Dunaeva et al., 2003; Merchant et al., 2004).

Human *SUFU* has been suggested to be a tumor suppressor gene based on the findings in a screen of 46 medulloblastoma tumors (Taylor et al., 2002). In 4 out of these 46 medulloblastomas, truncating mutations in the *SUFU* gene were found, of which 2 were germline mutations. However, in another screen of 145 primitive neuroectodermal tumors, including 134 medulloblastomas and 11 medulloblastoma-derived cell lines, no somatic or germline mutations in *SUFU* were found (Koch et al., 2004), suggesting that genetic alteration of *SUFU* is a relatively rare event in human medulloblastomas.

In *Drosophila*, loss-of-function mutation in *Su(fu)* suppresses the effects of mutations in *fu*, but, in the absence of other mutations, it results in essentially no altered phenotype (Ohlmeyer and Kalderon, 1998; Preat, 1992). In zebrafish, genetic ablation (Koudijs et al., 2005) or morpholino (MO) knockdown of *Sufu* revealed a relatively weak repressor activity in the Hh pathway accompanied by only slight upregulation of *Ptch1* expression (Tay et al., 2005; Wolff et al., 2003).

In order to gain insight into the role that Sufu plays in mammals, we have disrupted the *Sufu* gene in the mouse by using gene targeting in embryonic stem cells (ESCs), and we revealed an essential role for Sufu in the mammalian Hh signaling pathway, demonstrating a fundamental evolutionary divergence in regulation of Hh signaling.

Results

Sufu$^{-/-}$ Embryos Die In Utero at ~E9.5

To gain insight into the function of Sufu in mammals, homologous recombination in mouse ESCs was used to generate mice with a functional ablation of the *Sufu* gene (see the Supplemental Data available with this article online). Unexpectedly, embryos homozygous for the *Sufu* null allele die in utero around E9.5 and exhibit a severely deformed cephalic region that includes an open fore-, mid-, and hindbrain and neural tube (Figures 1D–1F). Compared to other mouse Hh pathway loss-of-function mutants, there is a striking similarity to

*Correspondence: rune.toftgard@biosci.ki.se (R.T.); stephan.teglund@biosci.ki.se (S.T.)

[4] These authors contributed equally to this work.

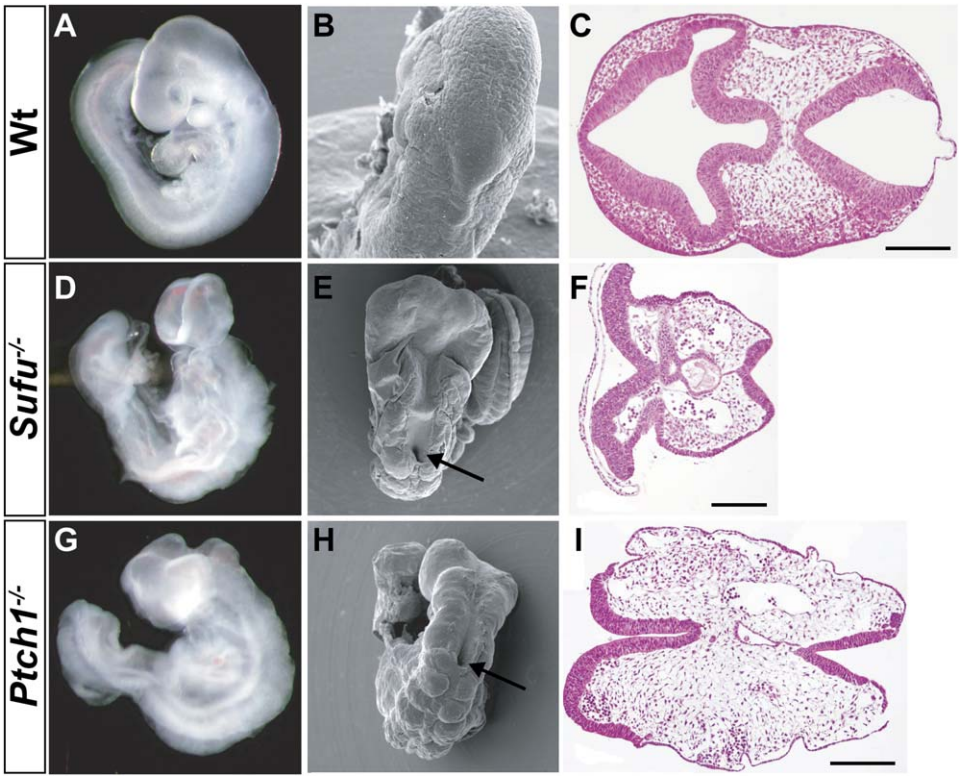

Figure 1. *Sufu*$^{-/-}$ Embryos Die In Utero at ~E9.5, and the Neural Tube and Cephalic Vesicles Fail to Completely Close

(A–I) (A, D, and G) Wild-type (wt), *Sufu*$^{-/-}$, and *Ptch1*$^{-/-}$ E9.5 embryos. (B, E, and H) SEM analysis showing the open hindbrain and the anterior neuropore (arrows) in the *Sufu*$^{-/-}$ and *Ptch1*$^{-/-}$ embryos. (C, F, and I) Formalin-fixed and hematoxylin-eosin-stained transverse sections from the cephalic region showing lack of closing and properly forming cephalic vesicles in both *Sufu*$^{-/-}$ and *Ptch1*$^{-/-}$ embryos. However, the anterior *Sufu*$^{-/-}$ neuroepithelium forms a wider, more open structure with considerably less mesenchymal tissue compared to the *Ptch1*$^{-/-}$ embryos. Anterior is to the left, and posterior is to the right. The scale bar is 100 μm.

Ptch1$^{-/-}$ embryos, which die around the same age and have similar morphology (Goodrich et al., 1997) (Figures 1G–1I). See the Supplemental Data for a detailed account of the morphological and histological findings.

Constitutive Activation of the Hh Pathway in the *Sufu*$^{-/-}$ Embryos

To investigate whether global changes in expression of Hh pathway components can be found in the *Sufu*$^{-/-}$ embryos, we used in situ hybridization on whole-mounts and sections in E8.5 (data not shown) and E9.5 embryos (Figure 2). Strikingly, there was a significant change in the expression pattern of both *Ptch1* and *Gli1*, particularly along the entire neural tube, where the expression domain was much broader and extended dorsally (Figures 2E, 2K, and 3N) compared to wild-type (wt) embryos (Figures 2D, 2J, and 3M). Moreover, the *Gli1* expression pattern was very similar in both *Sufu*$^{-/-}$ and *Ptch1*$^{-/-}$ embryos (Figures 2K and 2L). The expression of both *Gli2* and *Gli3* in the cephalic region was absent in the *Sufu*$^{-/-}$ embryos, consistent with the fact that the cephalic neural folds did not close (Figures 2N and 2Q). Besides the cephalic region, in the rest of the embryo, including the neural tube, there was a marked lower overall expression of *Gli3* (Figures 2Q and 3P). In contrast, particularly in the caudal region, *Gli2* expression remained detectable (Figure 2N). *Sufu* expression is normally rather widespread (Figure 2G), and no major changes occur in the *Ptch1*$^{-/-}$ embryos (Figure 2I), suggesting that *Sufu* is not itself a transcriptionally regulated Hh target gene.

Sufu$^{-/-}$ Embryos Develop a Ventralized Neural Tube

The role of Hh signaling activity in patterning of the dorsoventral aspects of the developing neural tube is well characterized (Briscoe and Ericson, 2001). Shh secreted from the notochord and floor plate forms a dorsoventral gradient that translates into a gradient of Gli activity. This, in turn, controls cell fate and the position of the different neuronal subtypes of the ventral neural tube (Stamataki et al., 2005). In *Ptch1*$^{-/-}$ embryos, the neural tube is ventralized (Goodrich et al., 1997). To gain insight into how loss of Sufu affects levels of Hh signaling, we investigated possible qualitative and/or quantitative differences in the patterning of the E9.5 *Sufu*$^{-/-}$ neural tube compared to *Ptch1*$^{-/-}$ and wt embryos.

FoxA2 (Hnf3β), a winged-helix transcription factor, is important for floor plate (FP) development in the neural tube and is also a marker, albeit not a definitive one, for FP cells (Placzek and Briscoe, 2005) (Figure 3D). In the *Sufu*$^{-/-}$ neural tube, FoxA2 was expressed along the entire dorsoventral axis (Figure 3E), suggesting that, like in *Ptch1*$^{-/-}$ embryos (Figure 3F), the neuroepithelium has adopted a ventralized identity. However, as shown by using the more definitive FP marker NK1R, a substance P receptor (data not shown), and *Nato3*

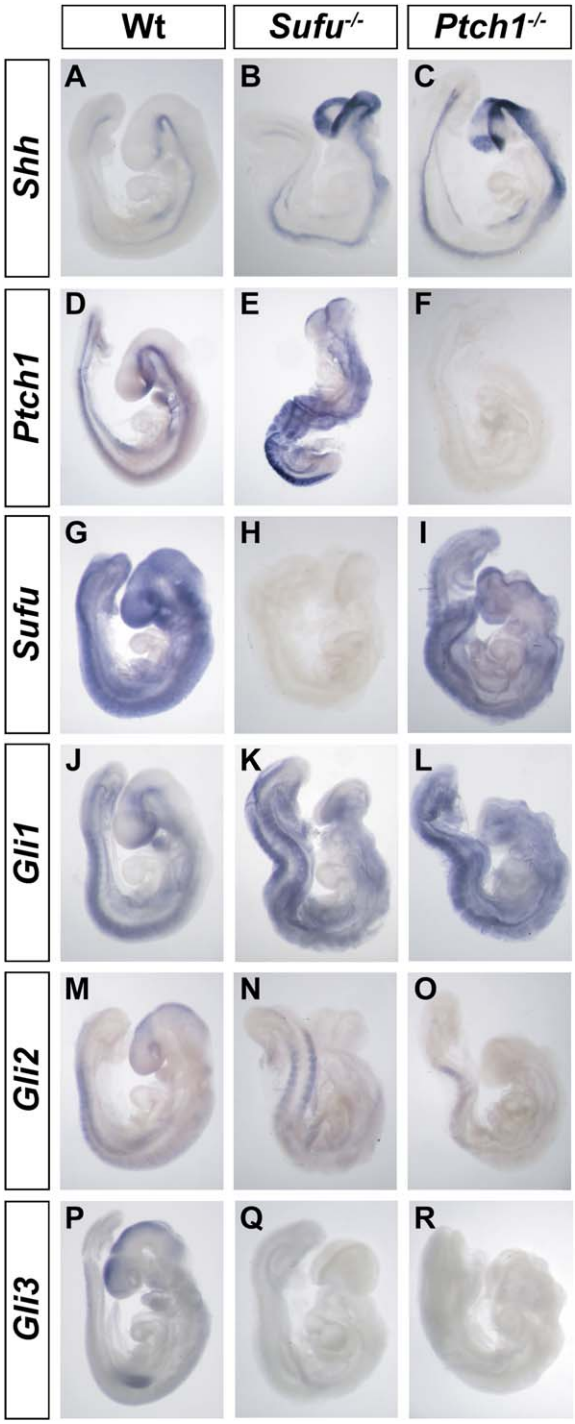

Figure 2. Ectopic Activation of Hh Target Genes and Aberrant Expression of Other Hh Pathway Components in *Sufu*$^{-/-}$ Embryos Mimicking that Seen in *Ptch1*$^{-/-}$ Embryos

(A–R) Whole-mount in situ hybridizations of wild-type (wt), *Sufu*$^{-/-}$, and *Ptch1*$^{-/-}$ E9.5 embryos with DIG-labeled antisense riboprobes against (A–C) *Shh*, (D–F) *Ptch1*, (G–I) *Sufu*, (J–L) *Gli1*, (M–O) *Gli2*, and (P–R) *Gli3*.

(Figure 3R), not all cells in the neural tube were bona fide FP cells. The FP cells normally express Shh (Placzek and Briscoe, 2005) (Figure 3A), regulated by a FP-specific enhancer in the *Shh* gene, which contains FoxA binding sites (Jeong and Epstein, 2003). Indeed, the expanded FoxA2 domain corresponded to the dorsal expansion of the Shh protein and mRNA expression (Figure 3B and Figure S3).

To understand whether the different neuronal subtypes were forming in the *Sufu*$^{-/-}$ neural tube, we immunostained for the Nkx2.2 and Nkx6.1 homedomain proteins, both of which were misexpressed along the entire dorsoventral axis (Figures 3H and 3K) compared to wt (Figures 3G and 3J), mirroring the expression seen in the *Ptch1*$^{-/-}$ neural tube (Figures 3I and 3L). The homedomain protein Isl1/2 is normally expressed in the motor neuron (MN) domain, and the number of Isl1/2 immunoreactive cells in the *Sufu*$^{-/-}$ (Figure 3E) and *Ptch1*$^{-/-}$ neural tube (Figure 3F) appears rather similar to wt (Figure 3D). However, in both mutants, the Isl1/2-positive cells are scattered along the dorsoventral axis rather than confined to the discrete MN domain. In contrast, the homedomain protein Pax6, normally expressed in the dorsal neural tube, was essentially lost in both *Sufu*$^{-/-}$ (Figure 3H) and *Ptch1*$^{-/-}$ (Figure 3I) compared to wt (Figure 3G). However, in the region of neural tube closure, *Ptch1*$^{-/-}$ mutants display Pax6 expression at the most dorsal region (data not shown), as has been described before (Bai et al., 2002). These data demonstrate that the *Sufu*$^{-/-}$ neural tube shows a strong ventralization, with most neuronal cells committed to a ventral fate.

The Constitutive Gli Activity in the *Sufu*$^{-/-}$ MEFs Is Unaffected by Either a Smoothened Agonist or Antagonist and Is Partially Sensitive to PKA Inhibition

To further explore the Sufu-dependent Hh signaling defects in more detail, we analyzed embryonic fibroblast (MEF) cell lines established from *Sufu*$^{+/+}$ (wt), *Sufu*$^{+/-}$, and *Sufu*$^{-/-}$ E9.5 embryos with the same genetic background. *Ptch1*$^{-/-}$ MEFs were used in comparison (Taipale et al., 2000). The expression of the Hh target genes *Ptch1*, *Gli1*, and, to some extent, *Ptch2* was upregulated in the *Sufu*$^{-/-}$ MEFs compared to the wt MEFs, as shown by RT-PCR (Figure 4A); this finding is consistent with the constitutively active Hh signaling seen in the embryos. A similar expression pattern was seen in the *Ptch1*$^{-/-}$ MEFs. *Gli2* and *Smo* expression remained unchanged in the *Sufu*$^{-/-}$ as well as the *Ptch1*$^{-/-}$ MEFs compared to wt. The absence of *Sufu* mRNA in the *Sufu*$^{-/-}$ MEFs was confirmed, and the expression of *Sufu* was not altered in the *Ptch1*$^{-/-}$ MEFs (Figure 4A).

To assess the activity of the Gli transcription factors in the MEFs, we used a luciferase assay with reporter plasmids containing eight wt (8×GliLuc) or mutant (8×Gli^{mut}Luc) Gli binding sites in tandem (Sasaki et al., 1997). Both *Sufu*$^{-/-}$ MEF lines #1 and #2 showed a similar ~12- to 15-fold increase in reporter activity relative to wt MEFs (Figure 4B). This increased activity is dependent on intact Gli binding sites since the 8×Gli^{mut}Luc reporter gave essentially no significant activity above that found in wt MEFs (Figure 4B).

We next asked if we could rescue the phenotype of the *Sufu*$^{-/-}$ MEF cells and repress the increased Gli activity by reintroducing Sufu. Transient transfection of human *SUFU* caused a reduction in Gli activity to wt levels (Figure 4B). This demonstrates that the observed phenotype is Sufu dependent and not due to other genetic

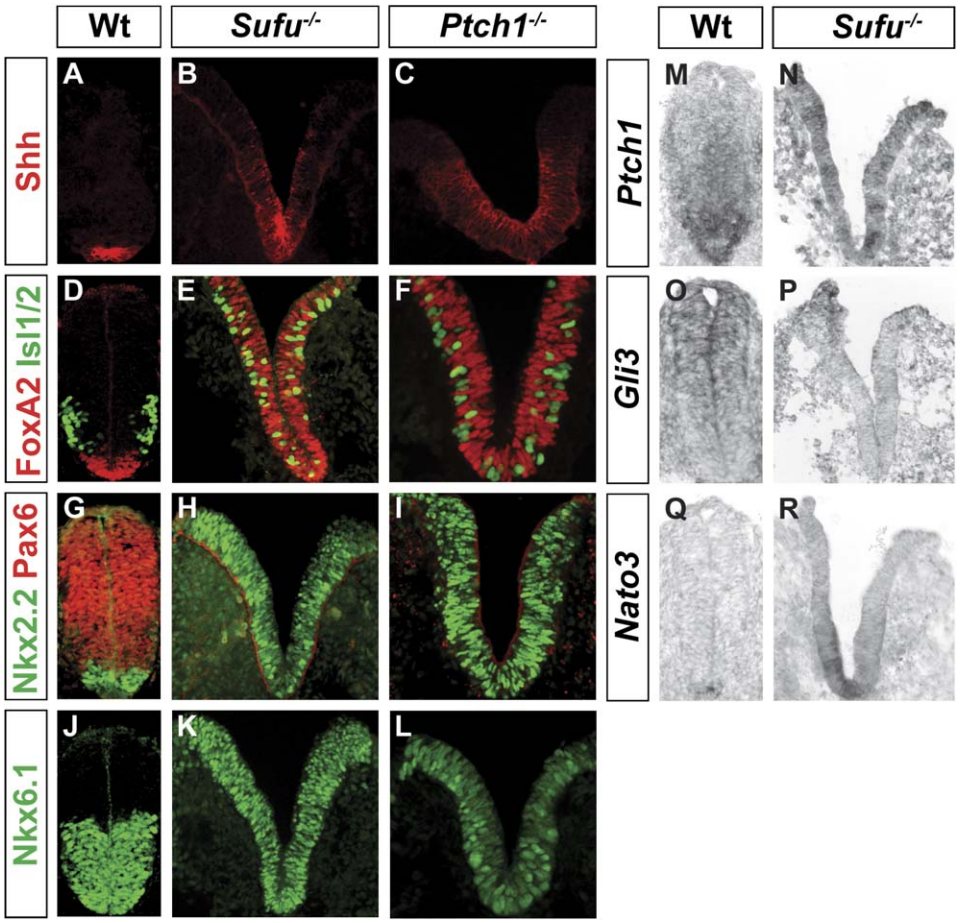

Figure 3. Ventralization of the *Sufu*$^{-/-}$ Embryonic Neural Tube Similar to that Seen in *Ptch1*$^{-/-}$ Embryos

(A–L) Transverse sections of the neural tube at the thoracic level of wild-type (wt), *Sufu*$^{-/-}$, and *Ptch1*$^{-/-}$ E9.5 embryos immunofluorescently stained with antibodies against (A–C) Shh (red), (D–F) FoxA2 (red) and Isl1/2 (green), (G–I) Nkx2.2 (green) and Pax6 (red), and (J–L) Nkx6.1 (green). (M–R) In situ hybridization of neural tube sections of wt and *Sufu*$^{-/-}$ E9.5 embryos hybridized with DIG-labeled riboprobes against (M and N) *Ptch1*, (O and P) *Gli3*, and (Q and R) *Nato3*.

alterations in the ES cells or MEF cells. Furthermore, it shows that human SUFU can functionally substitute for mouse Sufu.

To address the question of whether the observed Gli-mediated Hh signaling activity in the *Sufu*$^{-/-}$ MEF cells can be further stimulated, we incubated the *Sufu*$^{-/-}$ MEF cells with or without a concentration of Smo agonist (SAG) that has been shown to fully activate the Hh pathway (Chen et al., 2002). No further increase in Gli reporter activity could be observed (Figure 4C), suggesting that in the absence of Sufu, activation of Smo could not induce additional Gli-mediated transcriptional activity. Conversely, we tested whether cyclopamine, a known inhibitor of the Hh pathway that acts on Smo, could inhibit Gli reporter activity (Taipale et al., 2000). However, again, no effect was observed (Figure 4C), indicating that neither stimulation nor inhibition of the Hh pathway at the level of Smo has any significant effect on Gli activity in the absence of Sufu.

Protein kinase A (PKA) is known to negatively affect Hh signaling. To test whether PKA has such an effect in cells lacking Sufu, we treated MEF cells with forskolin, a known activator of PKA, and could inhibit the Gli-mediated response, but only by ~50% (Figure 4D). The same result was obtained by expressing a constitutively active form of the catalytic subunit of PKA. In contrast, an almost complete suppression was observed in the *Ptch1*$^{-/-}$ MEFs (Figure 4D), as has been shown before (Taipale et al., 2000). An inhibitor of PKA, H-89, as expected had no significant effect on the Gli response (Figure 4D).

EGFP::GLI1 Localizes Predominantly in the Cytoplasm of *Sufu*$^{-/-}$ MEFs

One of the proposed roles for Sufu is to retain Gli proteins in the cytoplasm. To determine the subcellular localization of GLI1 in the absence of Sufu, we transiently transfected the MEF cells with GLI1 fused to EGFP (EGFP::GLI1) to visualize the protein. EGFP::GLI1 localized predominantly in the cytoplasm of *Sufu*$^{-/-}$ MEFs, and no significant difference to wt and *Ptch1*$^{-/-}$ MEFs was observed (Figure 4E). Transfection of the parental EGFP plasmid gave a different localization pattern, which was both cytoplasmic and nuclear (Figure 4E), indicating that the localization we observed is GLI1 specific and not a property of the EGFP protein.

The nuclear export of Gli proteins is dependent on Crm1 (Kogerman et al., 1999), which facilitates the translocation

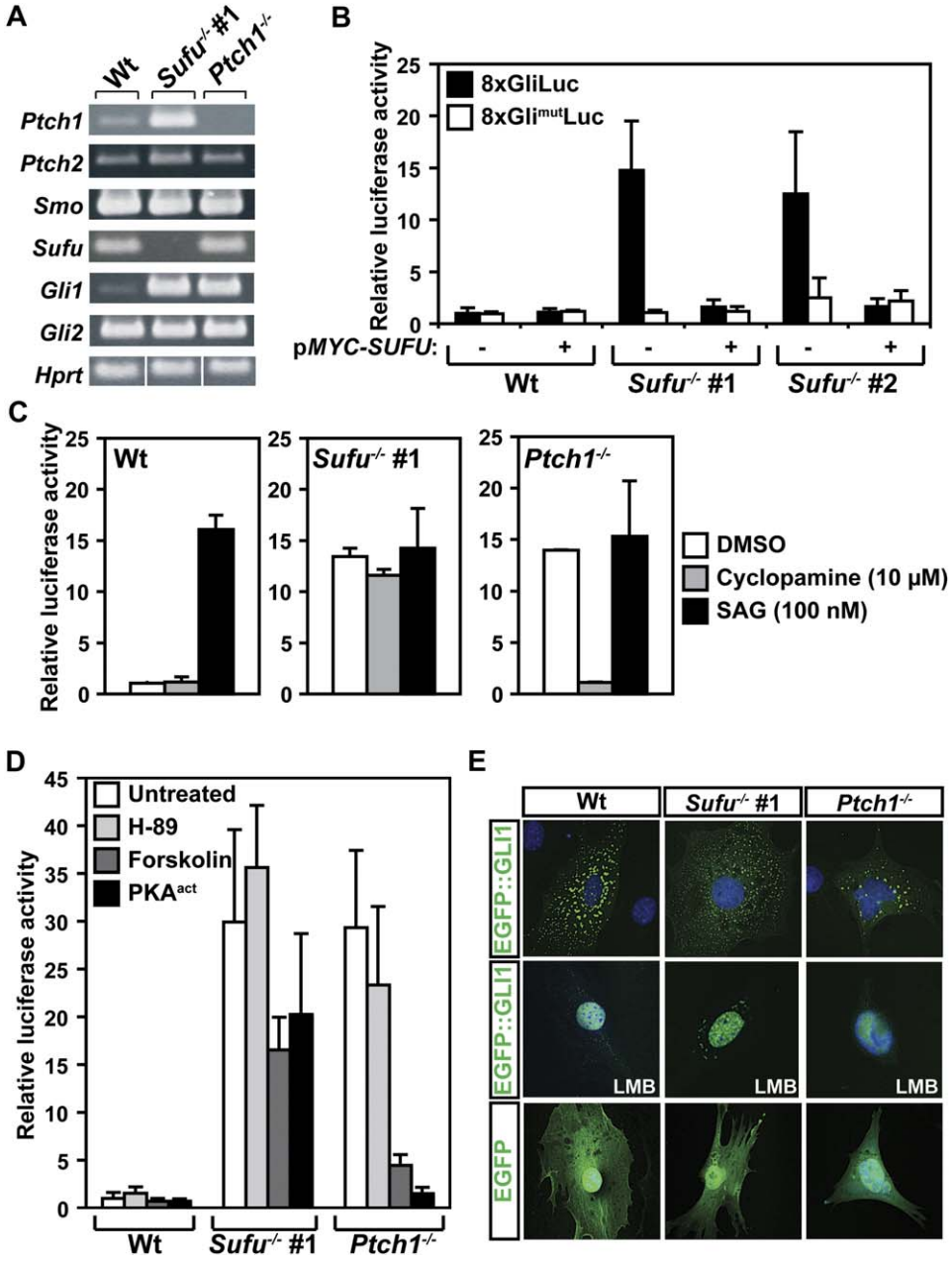

Figure 4. GLI1 Predominantly Resides in the Cytoplasm of *Sufu*$^{-/-}$ MEFs, Whose Constitutive Hh Pathway Activity Cannot Be Modulated at the Level of Smo and Can Be Partially Blocked by PKA

(A) Agarose gel analysis of RT-PCR reactions from *Sufu*$^{+/+}$ (wt), *Sufu*$^{-/-}$ cell line #1, and *Ptch1*$^{-/-}$ MEFs with primers specific for *Ptch1*, *Ptch2*, *Smo*, *Sufu*, *Gli1*, and *Gli2*. Primers for *Hprt* were used as a control for RNA input levels.

(B) Transient transfection of *Sufu* wt (+/+) and mutant (−/−) MEF lines #1 and #2 with 8×GliLuc (filled columns) or 8×Gli^{mut}Luc (open columns) luciferase reporter plasmids with (+) or without (−) the p*MYC-SUFU* expression plasmid. Gli reporter activity, which was given an arbitrary level of 1.0, is presented relative to wt MEFs after compensating for transfection efficiency by using the *Renilla* luciferase reporter plasmid. Results are means ± standard deviation (SD) of the mean of at least three independent experiments.

(C) Treatment of wt, *Sufu*$^{-/-}$ cell line #1, and *Ptch1*$^{-/-}$ MEFs with 10 μM cyclopamine (shaded column), 100 nM Smoothened agonist (SAG) (black column), or with DMSO alone (open column) for 2 days prior to measuring 8×GliLuc reporter activity. Results are means ± standard deviation (SD) of the mean of at least two independent experiments.

(D) Treatment of wt, *Sufu*$^{-/-}$ cell line #1, and *Ptch1*$^{-/-}$ MEFs with 1 μM of the PKA inhibitor H-89 (light shaded columns) and 100 μM forskolin (dark shaded column), transfected with a constitutively active PKA subunit expression plasmid (black column) or untreated (open column) for 1 day prior to measuring 8×GliLuc reporter activity. Results are means ± standard deviation (SD) of the mean of at least three independent experiments.

(E) Confocal images of wt, *Sufu*$^{-/-}$ cell line #1, and *Ptch1*$^{-/-}$ MEFs after transient transfection with expression plasmids for EGFP::GLI1 or EGFP alone for 24 hr with or without 10 ng/ml Leptomycin B (LMB) treatment for 6 hr. Nuclei are stained blue.

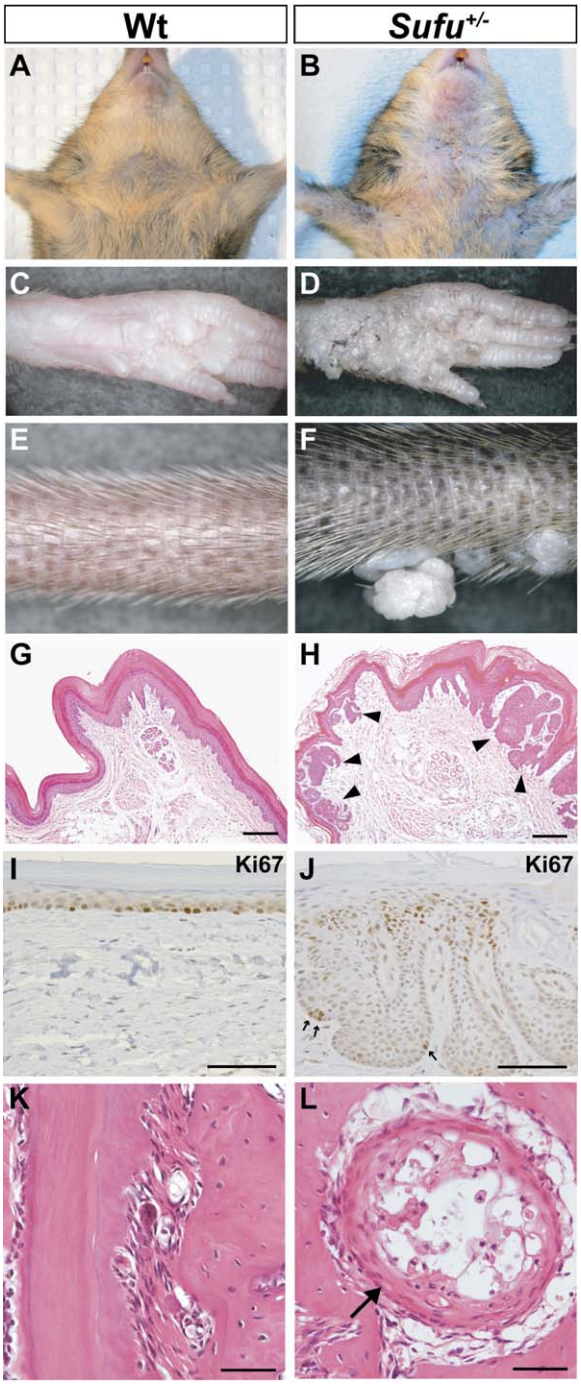

Figure 5. *Sufu*$^{+/-}$ Mice Develop a Skin Phenotype with Gorlin-like Features

(A and B) Ventral view of a wild-type (wt) and a *Sufu*$^{+/-}$ mouse, the latter showing alopecia and increased pigmentation.

(C and D) Paws from a wt and a *Sufu*$^{+/-}$ mouse, the latter displaying increased pigmentation and skin papules.

(E and F) Tails from a wt and a *Sufu*$^{+/-}$ mouse, the latter with increased pigmentation and skin nodules.

(G and H) Hematoxylin-eosin (H&E)-stained paw sections from a wt and a *Sufu*$^{+/-}$ mouse, the latter showing several epidermal basaloid proliferations (arrowheads). The scale bar is 100 μm.

(I and J) Paw tissue sections from a wt and a *Sufu*$^{+/-}$ mouse immunostained against Ki67, the latter demonstrating relatively few positive cells in the epidermal proliferations (arrows). The scale bar is 100 μm.

(K and L) H&E-stained jaw sections from a wt and a *Sufu*$^{+/-}$ mouse, the latter with a keratocyst (arrow). The scale bar is 50 μm. All mice are around 2 years of age.

of proteins with a nuclear export signal, a process that can be blocked by Leptomycin B (LMB). To investigate whether the cytoplasmic localization of GLI1 in the *Sufu*$^{-/-}$ MEFs is dependent on active nuclear export, we treated *EGFP::GLI1*-transfected MEFs with LMB and observed a strong nuclear retention of the EGFP::GLI1 fusion protein regardless of MEF genotype (Figure 4E). The control EGFP subcellular localization remained unchanged upon LMB treatment (data not shown).

Sufu$^{+/-}$ Mice Develop a Skin Phenotype with Gorlin-like Features

Having established that homozygous inactivation of *Sufu* in mouse embryos and MEFs results in constitutive and seemingly full activation of the Hh signaling pathway, we asked if any Hh-related phenotypic changes are present in *Sufu*$^{+/-}$ mice. Such mice are born at the expected Mendelian ratio, appear normal at birth, show normal growth, and are fully fertile.

However, a distinct skin phenotype with 100% penetrance (43/43 mice examined) developed in the *Sufu*$^{+/-}$ mice. This phenotype is macroscopically characterized by ventral alopecia (Figure 5B), increased pigmentation (Figures 5B, 5D, and 5F), and papules and nodules on the paws and tail (Figures 5D and 5F); is macroscopically visible from ~1.5 years of age; and becomes more severe in older mice. The earliest microscopic alterations were seen as small basaloid evaginations arising from the basal epidermal cells on the palmar aspect of the paws, at about 6 months of age. By 2 years of age, alterations were found in all skin areas (Figure 5H and Figures S5G and S5H). Immunohistochemical staining for the proliferation marker Ki67 revealed a relatively low number of positive cells (Figure 5J), consistent with the observed slow growth of these changes. Additional characterization of the skin phenotype can be found in the Supplemental Data. Furthermore, we frequently observed the appearance of mandibular keratocysts in the *Sufu*$^{+/-}$ mice (Figure 5L), which is a typical finding in Gorlin patients.

Overexpression of the Hh effectors GLI1 and Gli2 (Hutchin et al., 2005; Nilsson et al., 2000) as well as a constitutively active form of Smo (Grachtchouk et al., 2003) in mouse skin drives the development of a range of hair follicle-associated lesions with phenotypes correlating to different levels of Gli expression. To investigate whether increased Hh signaling is underlying the appearance of skin lesions in *Sufu*$^{+/-}$ mice, we measured the levels of *Gli1* expression by quantitative real-time PCR in the skin of ~2-year-old *Sufu*$^{+/-}$ and wt mice on a mixed B6;129 background. Three out of three tested *Sufu*$^{+/-}$ mice showed a 9.8- to 16.2-fold increase in *Gli1* mRNA levels compared to age-matched wt controls (Figure 6B). Moreover, in younger mice with less advanced proliferations, ~1 year old on a B6 congenic background (N7), smaller, but still significant, increases (4.2- to 9.6-fold) were found in four out of four *Sufu*$^{+/-}$ mice compared to wt control (Figure 6A). Thus, the increase in *Gli1* expression levels correlate with the extent

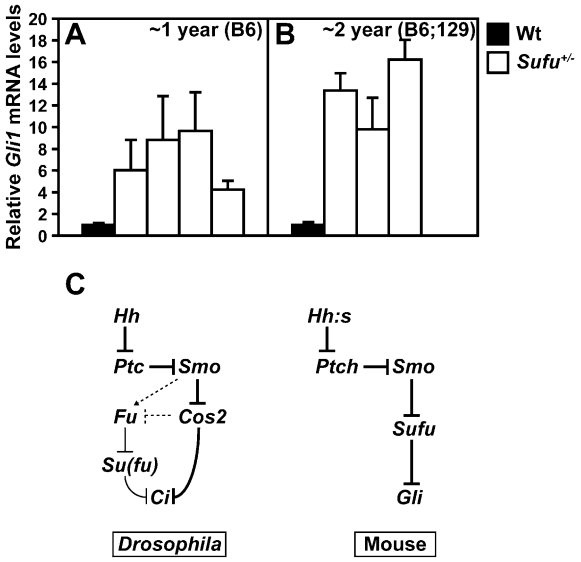

Figure 6. Skin from *Sufu*$^{+/-}$ Mice Express Increased Levels of *Gli1*, Indicative of an Active Hh Pathway, and Genetic Diagrams Depicting the Divergence of Core Components in the Pathway in Insects versus Mammals

(A and B) Real-time quantitative PCR for *Gli1* expression in wt (filled columns) and *Sufu*$^{+/-}$ (open columns) skin around (A) 1-year-old mice on a B6 genetic background (generation N7) or (B) 2-year-old mice on a mixed B6;129 background. *Gli1* expression is presented relative to wt skin, which was given an arbitrary level of 1.0, after normalizing the samples with the mouse *GAPDH* as an endogenous control. Results are means ± standard deviations of samples in triplicate.

(C) In *Drosophila*, the major pathway controlling Ci downstream of Smo is mediated via Cos2, while the pathway via Su(fu) has a less important role. In the mouse, a major postreceptor mechanism controlling Gli activity is mediated by Sufu, as we have demonstrated in this paper.

of the epidermal skin changes. A preliminary comparison of skin manifestations in heterozygous *Ptch1* and *Sufu* mice on the same genetic background reveals that the skin phenotype is tied to Sufu haploinsufficiency; very few *Ptch1*$^{+/-}$ mice developed these skin manifestations.

Discussion

In this study, we have addressed the role of Sufu in the mammalian Hh signaling pathway by using gene targeting in the mouse. Surprisingly, we found that *Sufu* knockouts are embryonic lethal and show strong similarities with *Ptch1* knockouts (Goodrich et al., 1997), and that Hh signaling is strongly activated in a ligand-independent manner in *Sufu*$^{-/-}$ cells. Moreover, *Sufu*$^{+/-}$ mice develop a skin phenotype with many features found in Gorlin syndrome. Furthermore, no support for a direct role of Sufu in the Wnt pathway was found (see the Supplemental Data).

Comparable Ligand-Independent Activation of Hh Signaling in *Sufu* and *Ptch1* Mutants

There is a remarkable agreement between the *Sufu*$^{-/-}$ and *Ptch1*$^{-/-}$ embryos in terms of the spatiotemporal expression pattern of all the markers examined both in the whole-mount embryo and neural tube analysis. High-level expression of the *Ptch1* and *Gli1* target genes in the *Sufu*$^{-/-}$ embryos suggests that Sufu is endowed with a strong repressor activity, removal of which causes ectopic activation of the Hh pathway. It should be emphasized that in the ventralized spinal cord from the *Sufu*$^{-/-}$ embryos, prominent ectopic expression of target genes such as FoxA2 and Nkx2.2, which require the highest levels of Hh signaling, is evident (Stamataki et al., 2005). Evidently, this high Hh activity is dominant in patterning the neural tube over the dorsalizing signals mediated by the Bmp proteins, which normally act in an antagonizing manner to Shh in the neural tube (Liem et al., 1995). Taken together, this indicates that mammalian Sufu, in striking contrast to the situation in *Drosophila*, is an equally strong repressor of the Hh pathway, as Ptch1 and removal of either one is sufficient to induce a similar high level of cell autonomous Hh signaling.

Recently, another study describing a different Sufu mutant allele was published (Cooper et al., 2005). Their homozygous mutant embryo phenotype generally agrees with ours in that the embryos die at the same stage with similar defects.

Mechanistic Insights into the Role of Mammalian Sufu

Based on studies of the effects of activators and inhibitors (SAG and cyclopamine, respectively) of Smo activity in the *Sufu*$^{-/-}$ MEFs, it appears that these cells have uncoupled the upstream ligand-dependent activation of Smo from the downstream Gli activity. This observation further suggests that constitutive activation of Hh signaling in cells lacking Sufu is determined by their intrinsic competence for Hh response and not actual exposure to Hh ligands. This independence of Hh ligand is further demonstrated in mouse *Sufu*$^{-/-}$; *Shh*$^{-/-}$ double mutant embryos, which appear morphologically similar to the *Sufu*$^{-/-}$ mutants (unpublished data). Additional support for this conclusion is presented in an accompanying paper (Varjosalo et al., 2006 [this issue of *Developmental Cell*]), where it is shown that downregulation of Sufu levels by RNAi in NIH-3T3 or *Smo*$^{-/-}$ cells results in activation of Hh signaling.

Activation of PKA inhibits Hh pathway activity in mammalian cells, and phosphorylation of T374 in Gli1, associated with modulation of the adjacent nuclear localization signal, was recently proposed to mediate at least part of this effect (Sheng et al., 2005). In *Ptch1*$^{-/-}$ MEFs, PKA activation effectively inhibited Gli reporter gene activity, whereas, in *Sufu*$^{-/-}$ MEFs, only partial inhibition was observed. This suggests that the full repressive effect of PKA activation on the Hh pathway is due to more than one mechanism and targets additional Hh pathway components.

From the proposed function for Sufu, one would have expected to see an increased nuclear accumulation of EGFP::GLI1 in the *Sufu*$^{-/-}$ MEFs. However, this is not evident from our data. On the contrary, the steady-state EGFP::GLI1 localization remains predominantly cytoplasmic and becomes nuclear only after the nuclear export process is blocked by LMB. This indicates that there is a highly effective shuttling of GLI1 protein out of the nucleus, and only when you block the nuclear export is there a detectable accumulation regardless of whether Sufu is present. We interpret these results to suggest that Sufu's primary role is not to retain GLI1 in

the cytoplasm, but rather to mediate repression of Gli-dependent transcription in the nucleus (Cheng and Bishop, 2002; Kogerman et al., 1999).

Evolutionary Divergent Role of Sufu in Hh Signaling

The severe functional consequences and the high level of Hh signaling caused by deleting the *Sufu* gene in the mouse was surprising given the overall conservation of the Hh pathway during evolution and the lack of an altered phenotype in the corresponding *Drosophila* mutants (Preat, 1992). Recently, another unanticipated result was revealed when a possible mouse ortholog of *Drosophila Fu* was targeted and no apparent Hh-dependent phenotypes during embryonic development were seen (Chen et al., 2005; Merchant et al., 2005). In contrast, *Drosophila fu* mutants are embryonic lethal (Preat et al., 1993), and, in zebrafish, MO knockdown of *Fu* abrogated Hh-dependent specification of myotome cell types (Wolff et al., 2003). Moreover, genetic inactivation (Koudijs et al., 2005) or MO knockdown of *Sufu* in zebrafish (Wolff et al., 2003) results in a detectable Hh-related phenotype, but the effect is much weaker than that caused by elimination of *Ptc*. In contrast, our data presented here indicate that, in the mouse, null mutations of *Sufu* and *Ptch1* produce equally strong perturbations of the Hh pathway. This suggests that not only has the Hh pathway evolved differently in vertebrates compared to invertebrates, but also within vertebrates, since mammals and teleosts show divergence in the pathway. Another such example of differences in the Hh pathway is illustrated by the recent finding that intraflagellar transport (IFT) proteins are required for transduction of the Hh signal in the mouse (Huangfu and Anderson, 2005; Huangfu et al., 2003; Liu et al., 2005), whereas analysis of IFT mutants in zebrafish (Sun et al., 2004; Tsujikawa and Malicki, 2004) and *Drosophila* (Han et al., 2003; Sarpal et al., 2003) did not reveal any Hh-dependent phenotypes. A model depicting the genetic interaction in mammals in comparison to the fly is shown in Figure 6C. This fundamental divergence in regulatory mechanisms has several important implications. In the fly, it is presently believed that Su(fu) together with the atypical kinesin Cos2 represent intracellular negative regulators of Hh signaling (Hooper and Scott, 2005) and that Cos2 plays a major role by tethering the transcriptional effector Ci to microtubules and, in the absence of ligand, promotes processing of Ci to its truncated repressor form. Upon ligand stimulation, a direct interaction between the C-terminal tail of Smo and Cos2 is enhanced, leading to inhibition of Ci processing and nuclear availability of activated full-length Ci. Su(fu), on the other hand, resides mostly in a separate intracellular complex also containing Ci (Lum et al., 2003; Stegman et al., 2000) and functions both to tether Ci in the cytoplasm and to inhibit activated full-length Ci (Methot and Basler, 2000; Wang et al., 2000). However, even in the absence of Su(fu), Cos2 is able to sequester Ci in the cytoplasm and maintain normal regulation of Hh signaling, whereas, in the absence of Cos2, constitutive activation of Ci ensues (Wang et al., 2000). In the mouse, Sufu loss alone leads to complete activation of the Hh signaling pathway, and mice therefore may not utilize a Cos2-like activity that in *Drosophila* is sufficient to maintain Hh pathway regulation in the absence of Sufu. Thus, when Sufu is removed, unrestrained Gli-mediated transcriptional activation is allowed by eliminating repression mechanisms normally inhibiting Gli activity. In mammalian cells, Gli1 and Gli2 serve mainly as positive transcriptional regulators, whereas Gli3 is processed and, for the most part, acts as a repressor (Ingham and McMahon, 2001). Since Sufu can interact with the N-terminal part of Gli proteins and the Sufu binding motif is retained in the Gli3 repressor form (Dunaeva et al., 2003), it appeared likely that Sufu also exerts a negative influence on the repressor activity of Gli3. Since we find a strong activation of Hh signaling in cells lacking Sufu in vivo and in vitro, we propose that Gli-mediated transcriptional activation is dominant over Gli-mediated repression. Alternatively, this result may be due to the fact that Sufu, in analogy to the situation with Gli1 (Merchant et al., 2004), must interact with two different domains on Gli3, one of which is missing in the Gli3 repressor form, to achieve effective repression. This result may also be due to differential expression domains for the activating and repressive Gli isoforms.

Sufu$^{+/-}$ Mice Develop Features of Gorlin Syndrome

The phenotypes we observe in the *Sufu*$^{+/-}$ mice are in good agreement with the proposed role of Sufu as a regulator of Hh signaling. In patients with Gorlin syndrome (nevoid basal cell carcinoma syndrome [NBCCS]; MIM #109400), an autosomal dominant disorder in which one mutated copy of *PTCH1* is inherited (Gorlin, 2004; Hahn et al., 1996; Johnson et al., 1996), jaw keratocysts and skin changes, mostly in the form of basal cell carcinomas (BCCs) and palmar/plantar pits, but also including basaloid follicular hamartomas (BFHs), (Oseroff et al., 2005) are typical and dominant lesions. In the aging *Sufu*$^{+/-}$ mice, basaloid skin changes, pit-like lesions in the paws, and jaw keratocysts all correspond to similar lesions found in Gorlin patients, although the skin changes appear more like BFHs than typical BCCs. Thus, the *Sufu*$^{+/-}$ mouse represents a valuable and complementing animal model of this human disease. The reason that the *Sufu*$^{+/-}$ mice do not get typical BCCs is possibly because the levels of Gli activity needed for BCCs to develop is not reached in the *Sufu*$^{+/-}$ skin due to the level of regulation still offered by the remaining wt *Sufu* allele. Support for this notion comes from mouse models in which the severity of skin alterations is linked to the level of Gli activity (Grachtchouk et al., 2003; Nilsson et al., 2000). Similarly, BCCs do not develop spontaneously in the *Ptch1*$^{+/-}$ mice unless they are irradiated with UV light or ionizing radiation (Aszterbaum et al., 1999). In fact, the observed skin changes are more prominent in the *Sufu*$^{+/-}$ mice than in the *Ptch1*$^{+/-}$ mice (data not shown). The observation that the skin lesions express K17 and that we see the appearance of abortive hair follicle formation suggest that there is an expansion of primitive progenitor cells, a concept that is in line with data from studies of mice conditionally expressing Gli2 in the skin (Hutchin et al., 2005). In the few human patients reported with germline mutations in *SUFU*, no skin phenotypes were reported, possibly due to the patients' young age or the nature of mutations (Taylor et al., 2002). However, differential penetrance of this phenotype between mice and humans remains a possibility.

In the study of Cooper et al. (2005), contrary to our findings, no phenotypic changes in the heterozygous Sufu mutant mice were observed. One possible explanation could be mouse strain background differences since we differ in the 129 substrain used (129X1/SvJ versus 129S1/Sv) and in the source of C57BL/6 (Jackson Laboratories versus Charles River). Another possible explanation concerns how the alleles were targeted; we have deleted exon 1 along with the promoter, and Cooper et al. (2005) have deleted part of exon 7. It cannot formally be excluded that a C-terminally truncated Sufu protein is being made from the mutant allele reported by Cooper et al. (2005). If such a truncated protein has some residual activity, this may be enough to rescue the heterozygous (but apparently not the homozygous) mutant phenotype that we observe. In fact, a recent study reports that the N-terminal part of Sufu is sufficient to inhibit Gli-dependent transcription (Barnfield et al., 2005).

Concluding Remarks

The results presented in this study highlight an important evolutionary divergence in the basic regulatory circuits controlling Hh signaling, a pathway having a key role in development and human disease, including cancer, thereby illustrating the need to understand in detail the function of the pathway in mammalian systems. The unanticipated role of Sufu as a specific and potent repressor of Hh signaling also opens new therapeutic avenues to control deregulated Hh pathway activation, for example, by development of Sufu mimetics.

Experimental Procedures

Mouse Strains

Generation of the *Sufu* mutant mouse strain is described in the Supplemental Data, and this strain was provisionally designated B6;129X1/SvJ-*Sufu*^{tm1Rto}. The *Ptch1* knockout mice (B6;129-*Ptch1*^{tm1Mps}) were obtained from The Jackson Laboratory (stock 003081). The mice were housed in an SPF barrier facility according to local and national regulations, and conditions were approved by the Stockholm South Animal Ethics Committee.

Generation of MEF Cell Lines

Immortalized mouse embryo fibroblast (MEF) cell lines were established by using a 3T3-like protocol (Todaro and Green, 1963). Briefly, E9.5 embryos were incubated for 5 min in 0.05% trypsin-EDTA (Invitrogen) at 37ºC, medium was added, embryos were resuspended before plating onto tissue culture dishes and were passaged until crisis, and, eventually, immortal cells appeared. The MEF medium consisted of D-MEM (high glucose, w/o sodium pyruvate), heat-inactivated 10% fetal bovine serum (FBS), 2 mM L-glutamine, 1 mM sodium pyruvate, and 10 μg/ml gentamicin, all from Invitrogen. The *Ptch1*$^{-/-}$ MEFs, derived in a similar manner, were a kind gift from Dr J. Taipale, University of Helsinki, Finland.

Northern Blot Analysis, RT-PCR, and Real-Time Quantitative PCR

For the Northern analysis, total RNA from E8.5 and E9.5 embryos were prepared by using the RNeasy kit (Qiagen). Embryos were collected in RNAlater (Ambion) prior to preparation. For the Northern gel, 15 μg total RNA per lane was separated on a 1% formaldehyde-containing agarose gel and was transferred to Nytran Supercharge membranes (Schleicher & Schuell) in NorthernMax transfer buffer (Ambion) followed by UV crosslinking. The radioactively labeled probes consisted of a 1.2 kb mouse *Sufu* cDNA XhoI/NotI fragment from an EST clone (GenBank accession number AA754906) and a 1076 bp mouse *β-actin* cDNA fragment (Ambion). Prehybridizations were conducted for 1–2 hr, and hybridizations were conducted for 2–3 hr at 65ºC in ULTRAhyb (Ambion), followed by three washes at 65ºC in Low Stringency Buffer 1 (Ambion) and two washes at 65ºC in High Stringency Buffer 2 (Ambion).

For the RT-PCR analysis, total RNA from confluent MEF cells or embryos (*Actr1a* analysis) were prepared as described above with RNase-free DNaseI (Qiagen) treatment and were reverse transcribed into cDNA by using SuperScript (Invitrogen). PCR amplifications were performed with primers against mouse *Ptch1*, *Ptch2*, *Smo*, *Sufu*, *Gli1*, *Gli2*, *Actr1a*, *Hprt*, and *Actr1a* (see the Supplemental Data, Table S1).

For the real-time quantitative PCR, total RNA from fresh ~1-year-old *Sufu*$^{+/+}$ and *Sufu*$^{+/-}$ skin tissue on a B6 congenic background (N7) or frozen ~2-year-old *Sufu*$^{+/+}$ and *Sufu*$^{+/-}$ skin tissue on a mixed B6;129 background were prepared (Chomczynski and Sacchi, 1987). The RNA samples were treated with RNase-Free DNaseI (Promega) and were reverse transcribed with SuperScript (Invitrogen) with oligo(dT)$_{15}$ primers. The reactions were made up in TaqMan Universal PCR master mix (Applied Biosystems) with TaqMan Gene Expression Assays for mouse *Gli1* (assay ID #Mm00494645_m1) and endogenous control mouse *GAPDH* (#4352339E) and were analyzed on an ABI PRISM 7700 Sequence Detection System (Applied Biosystems). Samples were analyzed in triplicate for each dilution and were normalized to *GAPDH* in each sample before calculating relative *Gli1* mRNA levels.

Western Blot Analysis and ECL Detection

Total cell lysates from E9.5 embryos pooled according to genotype were prepared in extraction buffer (pH 7.6 at 4ºC containing 1% Triton X-100, 10 mM Tris-HCl, 5 mM EDTA, 50 mM NaCl, 30 mM Na-pyrophosphate, 50 mM NaF, 1 mM Na_3VO_4, 10% glycerol, and complete protease inhibitor cocktail [Roche]). The Triton X-100 was added after tissue homogenization by using an Ultra-Turrax T8 (IKA). Protein extracts were quantified with the DC protein assay (Bio-Rad). A total of 15 μg total protein per genotype and lane in 1× Laemmli sample buffer was separated on an 8% SDS-PAGE gel by using a Protean II xi Cell (Bio-Rad) and was transferred to a Hybond-ECL membrane (Amersham Biosciences) with a Trans-Blot apparatus (Bio-Rad). The protein membrane was subjected to ECL analysis (Amersham Biosciences) by using a primary polyclonal antibody against Sufu (1:200, sc-10933, Santa Cruz Biotechnology) and a secondary bovine α-goat IgG-HRP (1:2000, sc-2350, Santa Cruz Biotechnology). The chemiluminescent reaction was detected on Hyperfilm ECL (Amersham Biosciences). After stripping the membrane, protein loading was verified by using a primary monoclonal β-actin antibody (1:5000, A5441, Sigma) and a secondary sheep α-mouse IgG-HRP (1:5000, NA-931, Amersham Biosciences).

Scanning Electron Microscopy, In Situ Hybridizations, and Histochemistry

For the scanning electron microscopy, embryos were fixed in 2% glutaraldehyde, dehydrated in ascending concentrations of ethanol, dried by critical point, and mounted on aluminum stubs. After coating with 15 nm platinum, the samples were analyzed in a Jeol JSM-820 scanning electron microscope operating at 15 kV.

Whole-mount in situ hybridization was performed on E8.5 and E9.5 paraformaldehyde-fixed embryos (Henrique et al., 1995). Mouse antisense and sense (control) RNA probes were prepared by using DIG RNA labeling mix (Roche) together with T3, T7, or SP6 RNA polymerases (Roche). The linearized plasmids used as templates for the in vitro transcription were mouse cDNA fragments for *Shh* (0.6 kb in pBS II KS+), *Ptch1* (841 bp in pBS II KS+), *Sufu* (987 bp in pBS SK-), *Gli1* (552 bp in pBS II KS+), *Gli2* (1.0 kb in pBS II KS+), *Gli3* (1.1 kb in pBS II SK+), and *Axin2/Conductin* (637 bp in pBS II SK+). The Shh-hybridized embryos were paraffin embedded and sectioned.

Immunohistochemical localization of proteins in the neural tube was performed as described (Briscoe et al., 2000; Yamada et al., 1993). Antibodies against Shh, Nkx2.2, FoxA2, and Pax6 were obtained from the Developmental Studies Hybridoma Bank. The Nkx6.1 (Jensen et al., 1996) and Isl1/2 antibodies (Thor et al., 1991) have been described. NK1R antisera (s8305, Sigma) were a kind gift from Dr. G. Fortin, France. Images were collected with a Zeiss LSM510 confocal microscope.

In situ hybridization of neural tube sections was performed as described (Schaeren-Wiemers and Gerfin-Moser, 1993) by using DIG-labeled cRNA probes for mouse *Ptch1*, *Gli3*, and *Nato3* (Segev et al., 2001).

For the histological analysis, embryos and adult mouse tissue were fixed in 10% neutral-buffered formalin (Sigma) or Bouin's solution (Sigma), and they were subsequently paraffin embedded, sectioned at 4–5 μm, and stained with hematoxylin-eosin or followed by immunohistochemistry (see the Supplemental Data).

Luciferase Reporter Assays

For the luciferase reporter assays, 20,000 MEF cells were seeded into each well of a 24-well plate in MEF medium. The following day, cells were transfected with FuGENE 6 (Roche) with 300 ng of the luciferase reporter plasmids 8×GliLuc and 8×Gli^{mut}Luc (Sasaki et al., 1997) with or without 300 ng of the pMYC-*SUFU* expression plasmid (Kogerman et al., 1999), 300 ng of a constitutively active PKA catalytic subunit expression plasmid (Taipale et al., 2000), or 300 ng of the TOPflash and FOPflash reporter plasmids (Upstate Biotechnology), together with 50 ng of the *Renilla* luciferase phRL-TK reporter (Promega) to monitor the transfection efficiency. Two days after transfection, the medium was changed to low serum (0.5% FBS) with or without 10 μM cyclopamine in DMSO (Toronto Research Chemicals, Inc.), 100 nM Smoothened agonist (SAG) in methanol (provided by Dr J. Bergman, Karolinska Institutet, Sweden), 100 μM forskolin (Sigma) in DMSO, 1 μM H-89 (Sigma) in DMSO, or with DMSO alone and was incubated for 1–3 days before the cells were assayed with the Dual-Reporter Luciferase system (Promega) and the samples were analyzed on a Luminoskan Ascent microplate luminometer (Thermo Electron Corp.). The assays were conducted in triplicate and repeated at least three times. The values were normalized to the *Renilla* reporter before calculating relative levels.

GLI1 Subcellular Localization in MEFs

Wt, *Sufu*$^{-/-}$, and *Ptch1*$^{-/-}$ MEFs (1 × 10^6 cells) were each transfected with 5 μg of the expression constructs containing *GLI1* cDNA fused in frame 3′ of *EGFP* (*EGFP::GLI1* [Kogerman et al., 1999]) or with the parental *EGFP* plasmid alone (BD Biosciences Clontech) in MEF 1 solution by using Nucleofector technology, program T-20 (Amaxa Biosystems), and cells were seeded onto slide chambers, followed by culturing overnight. Twenty-four hours after transfection, cells were either treated with 10 ng/ml Leptomycin B (Sigma) for 3–6 hr or left untreated, washed in PBS, fixed in 4% PFA, washed in PBS again, and incubated with DRAQ5 (Alexis Biochemicals) for visualization of cell nuclei, followed by mounting with ProLong Gold antifade reagent (Invitrogen). Fluorescence was visualized with a Zeiss LSM510 confocal microscope with lasers set at 488 nm for EGFP and at 633 nm for DRAQ5.

Supplemental Data

Supplemental Data including Supplemental Results, Supplemental Experimental Procedures, five figures, one table, and references are available at http://www.developmentalcell.com/cgi/content/full/10/2/187/DC1/.

Acknowledgments

We thank B.-M. Skog, G. Brolin, A. Kisana, and J. Inzunza at the Karolinska Center for Transgene Technologies (KCTT); Kjell Hultenby at the Unit for Electron Microscopy (EMil); C. Lundmark and S. Warner for technical assistance; and J. Taipale for critical reading of the manuscript. This work was supported by grants from the Swedish Cancer Society, National Institutes of Health Program Project Grant AR47898, and National Institutes of Health/National Cancer Institute Mouse Models of Human Cancers Consortium Grant U01 CA105491. B.R. was supported by Wallenberg Consortium North (WCN). M.L. was supported by a postdoctoral fellowship from the Wenner-Gren Foundations, Stockholm, Sweden. J.E. was supported by the Royal Swedish Academy of Sciences by a donation from the Wallenberg Foundation, the Swedish Foundation for Strategic Research, the Swedish National Research Council, the Karolinska Institutet and the European Commission network grants Brainstem Genetics QLRT-2000-01467 and Stembridge QLG3-CT-2002-01141.

Received: August 19, 2005
Revised: November 28, 2005
Accepted: December 27, 2005
Published: February 6, 2006

References

Aszterbaum, M., Epstein, J., Oro, A., Douglas, V., LeBoit, P.E., Scott, M.P., and Epstein, E.H., Jr. (1999). Ultraviolet and ionizing radiation enhance the growth of BCCs and trichoblastomas in patched heterozygous knockout mice. Nat. Med. *5*, 1285–1291.

Bai, C.B., Auerbach, W., Lee, J.S., Stephen, D., and Joyner, A.L. (2002). Gli2, but not Gli1, is required for initial Shh signaling and ectopic activation of the Shh pathway. Development *129*, 4753–4761.

Barnfield, P.C., Zhang, X., Thanabalasingham, V., Yoshida, M., and Hui, C.C. (2005). Negative regulation of Gli1 and Gli2 activator function by Suppressor of fused through multiple mechanisms. Differentiation *73*, 397–405.

Briscoe, J., and Ericson, J. (2001). Specification of neuronal fates in the ventral neural tube. Curr. Opin. Neurobiol. *11*, 43–49.

Briscoe, J., Pierani, A., Jessell, T.M., and Ericson, J. (2000). A homeodomain protein code specifies progenitor cell identity and neuronal fate in the ventral neural tube. Cell *101*, 435–445.

Chen, J.K., Taipale, J., Young, K.E., Maiti, T., and Beachy, P.A. (2002). Small molecule modulation of Smoothened activity. Proc. Natl. Acad. Sci. USA *99*, 14071–14076.

Chen, M.H., Gao, N., Kawakami, T., and Chuang, P.T. (2005). Mice deficient in the fused homolog do not exhibit phenotypes indicative of perturbed hedgehog signaling during embryonic development. Mol. Cell. Biol. *25*, 7042–7053.

Cheng, S.Y., and Bishop, J.M. (2002). Suppressor of Fused represses Gli-mediated transcription by recruiting the SAP18-mSin3 corepressor complex. Proc. Natl. Acad. Sci. USA *99*, 5442–5447.

Chomczynski, P., and Sacchi, N. (1987). Single-step method of RNA isolation by acid guanidinium thiocyanate-phenol-chloroform extraction. Anal. Biochem. *162*, 156–159.

Cooper, A.F., Yu, K.P., Brueckner, M., Brailey, L.L., Johnson, L., McGrath, J.M., and Bale, A.E. (2005). Cardiac and CNS defects in a mouse with targeted disruption of suppressor of fused. Development *132*, 4407–4417.

Dunaeva, M., Michelson, P., Kogerman, P., and Toftgard, R. (2003). Characterization of the physical interaction of Gli proteins with SUFU proteins. J. Biol. Chem. *278*, 5116–5122.

Goodrich, L.V., Milenkovic, L., Higgins, K.M., and Scott, M.P. (1997). Altered neural cell fates and medulloblastoma in mouse patched mutants. Science *277*, 1109–1113.

Gorlin, R.J. (2004). Nevoid basal cell carcinoma (Gorlin) syndrome. Genet. Med. *6*, 530–539.

Grachtchouk, V., Grachtchouk, M., Lowe, L., Johnson, T., Wei, L., Wang, A., de Sauvage, F., and Dlugosz, A.A. (2003). The magnitude of hedgehog signaling activity defines skin tumor phenotype. EMBO J. *22*, 2741–2751.

Hahn, H., Wicking, C., Zaphiropoulous, P.G., Gailani, M.R., Shanley, S., Chidambaram, A., Vorechovsky, I., Holmberg, E., Unden, A.B., Gillies, S., et al. (1996). Mutations of the human homolog of *Drosophila* patched in the nevoid basal cell carcinoma syndrome. Cell *85*, 841–851.

Han, Y.G., Kwok, B.H., and Kernan, M.J. (2003). Intraflagellar transport is required in *Drosophila* to differentiate sensory cilia but not sperm. Curr. Biol. *13*, 1679–1686.

Henrique, D., Adam, J., Myat, A., Chitnis, A., Lewis, J., and Ish-Horowicz, D. (1995). Expression of a Delta homologue in prospective neurons in the chick. Nature *375*, 787–790.

Hooper, J.E., and Scott, M.P. (2005). Communicating with Hedgehogs. Nat. Rev. Mol. Cell Biol. *6*, 306–317.

Huangfu, D., and Anderson, K.V. (2005). Cilia and Hedgehog responsiveness in the mouse. Proc. Natl. Acad. Sci. USA *102*, 11325–11330.

Huangfu, D., Liu, A., Rakeman, A.S., Murcia, N.S., Niswander, L., and Anderson, K.V. (2003). Hedgehog signalling in the mouse requires intraflagellar transport proteins. Nature *426*, 83–87.

Hutchin, M.E., Kariapper, M.S., Grachtchouk, M., Wang, A., Wei, L., Cummings, D., Liu, J., Michael, L.E., Glick, A., and Dlugosz, A.A. (2005). Sustained Hedgehog signaling is required for basal cell carcinoma proliferation and survival: conditional skin tumorigenesis recapitulates the hair growth cycle. Genes Dev. *19*, 214–223.

Ingham, P.W., and McMahon, A.P. (2001). Hedgehog signaling in animal development: paradigms and principles. Genes Dev. *15*, 3059–3087.

Jensen, J., Serup, P., Karlsen, C., Nielsen, T.F., and Madsen, O.D. (1996). mRNA profiling of rat islet tumors reveals nkx 6.1 as a β-cell-specific homeodomain transcription factor. J. Biol. Chem. *271*, 18749–18758.

Jeong, Y., and Epstein, D.J. (2003). Distinct regulators of Shh transcription in the floor plate and notochord indicate separate origins for these tissues in the mouse node. Development *130*, 3891–3902.

Johnson, R.L., Rothman, A.L., Xie, J., Goodrich, L.V., Bare, J.W., Bonifas, J.M., Quinn, A.G., Myers, R.M., Cox, D.R., Epstein, E.H., Jr., and Scott, M.P. (1996). Human homolog of patched, a candidate gene for the basal cell nevus syndrome. Science *272*, 1668–1671.

Koch, A., Waha, A., Hartmann, W., Milde, U., Goodyer, C.G., Sorensen, N., Berthold, F., Digon-Sontgerath, B., Kratzschmar, J., Wiestler, O.D., and Pietsch, T. (2004). No evidence for mutations or altered expression of the Suppressor of Fused gene (SUFU) in primitive neuroectodermal tumours. Neuropathol. Appl. Neurobiol. *30*, 532–539.

Kogerman, P., Grimm, T., Kogerman, L., Krause, D., Unden, A.B., Sandstedt, B., Toftgard, R., and Zaphiropoulos, P.G. (1999). Mammalian suppressor-of-fused modulates nuclear-cytoplasmic shuttling of Gli-1. Nat. Cell Biol. *1*, 312–319.

Koudijs, M.J., den Broeder, M.J., Keijser, A., Wienholds, E., Houwing, S., van Rooijen, E.M., Geisler, R., and van Eeden, F.J. (2005). The zebrafish mutants dre, uki, and lep encode negative regulators of the Hedgehog signaling pathway. PLoS Genet. *1*, e19.

Liem, K.F., Jr., Tremml, G., Roelink, H., and Jessell, T.M. (1995). Dorsal differentiation of neural plate cells induced by BMP-mediated signals from epidermal ectoderm. Cell *82*, 969–979.

Liu, A., Wang, B., and Niswander, L.A. (2005). Mouse intraflagellar transport proteins regulate both the activator and repressor functions of Gli transcription factors. Development *132*, 3103–3111.

Lum, L., and Beachy, P.A. (2004). The Hedgehog response network: sensors, switches, and routers. Science *304*, 1755–1759.

Lum, L., Zhang, C., Oh, S., Mann, R.K., von Kessler, D.P., Taipale, J., Weis-Garcia, F., Gong, R., Wang, B., and Beachy, P.A. (2003). Hedgehog signal transduction via Smoothened association with a cytoplasmic complex scaffolded by the atypical kinesin, Costal-2. Mol. Cell *12*, 1261–1274.

Merchant, M., Vajdos, F.F., Ultsch, M., Maun, H.R., Wendt, U., Cannon, J., Desmarais, W., Lazarus, R.A., de Vos, A.M., and de Sauvage, F.J. (2004). Suppressor of fused regulates Gli activity through a dual binding mechanism. Mol. Cell. Biol. *24*, 8627–8641.

Merchant, M., Evangelista, M., Luoh, S.M., Frantz, G.D., Chalasani, S., Carano, R.A., van Hoy, M., Ramirez, J., Ogasawara, A.K., McFarland, L.M., et al. (2005). Loss of the serine/threonine kinase fused results in postnatal growth defects and lethality due to progressive hydrocephalus. Mol. Cell. Biol. *25*, 7054–7068.

Methot, N., and Basler, K. (2000). Suppressor of fused opposes hedgehog signal transduction by impeding nuclear accumulation of the activator form of Cubitus interruptus. Development *127*, 4001–4010.

Nilsson, M., Unden, A.B., Krause, D., Malmqwist, U., Raza, K., Zaphiropoulos, P.G., and Toftgard, R. (2000). Induction of basal cell carcinomas and trichoepitheliomas in mice overexpressing GLI-1. Proc. Natl. Acad. Sci. USA *97*, 3438–3443.

Ohlmeyer, J.T., and Kalderon, D. (1998). Hedgehog stimulates maturation of Cubitus interruptus into a labile transcriptional activator. Nature *396*, 749–753.

Oseroff, A.R., Shieh, S., Frawley, N.P., Cheney, R., Blumenson, L.E., Pivnick, E.K., and Bellnier, D.A. (2005). Treatment of diffuse basal cell carcinomas and basaloid follicular hamartomas in nevoid basal cell carcinoma syndrome by wide-area 5-aminolevulinic acid photodynamic therapy. Arch. Dermatol. *141*, 60–67.

Placzek, M., and Briscoe, J. (2005). The floor plate: multiple cells, multiple signals. Nat. Rev. Neurosci. *6*, 230–240.

Preat, T. (1992). Characterization of Suppressor of fused, a complete suppressor of the fused segment polarity gene of *Drosophila melanogaster*. Genetics *132*, 725–736.

Preat, T., Therond, P., Limbourg-Bouchon, B., Pham, A., Tricoire, H., Busson, D., and Lamour-Isnard, C. (1993). Segmental polarity in *Drosophila melanogaster*: genetic dissection of fused in a Suppressor of fused background reveals interaction with costal-2. Genetics *135*, 1047–1062.

Sarpal, R., Todi, S.V., Sivan-Loukianova, E., Shirolikar, S., Subramanian, N., Raff, E.C., Erickson, J.W., Ray, K., and Eberl, D.F. (2003). *Drosophila* KAP interacts with the kinesin II motor subunit KLP64D to assemble chordotonal sensory cilia, but not sperm tails. Curr. Biol. *13*, 1687–1696.

Sasaki, H., Hui, C., Nakafuku, M., and Kondoh, H. (1997). A binding site for Gli proteins is essential for HNF-3β floor plate enhancer activity in transgenics and can respond to Shh in vitro. Development *124*, 1313–1322.

Schaeren-Wiemers, N., and Gerfin-Moser, A. (1993). A single protocol to detect transcripts of various types and expression levels in neural tissue and cultured cells: in situ hybridization using digoxigenin-labelled cRNA probes. Histochemistry *100*, 431–440.

Segev, E., Halachmi, N., Salzberg, A., and Ben-Arie, N. (2001). Nato3 is an evolutionarily conserved bHLH transcription factor expressed in the CNS of *Drosophila* and mouse. Mech. Dev. *106*, 197–202.

Sheng, T., Chi, S., Zhang, X., and Xie, J. (2005). Regulation of Gli1 localization by the cAMP/PKA signaling axis through a site near the nuclear localization signal. J. Biol. Chem. *281*, 9–12.

Stamataki, D., Ulloa, F., Tsoni, S.V., Mynett, A., and Briscoe, J. (2005). A gradient of Gli activity mediates graded Sonic Hedgehog signaling in the neural tube. Genes Dev. *19*, 626–641.

Stegman, M.A., Vallance, J.E., Elangovan, G., Sosinski, J., Cheng, Y., and Robbins, D.J. (2000). Identification of a tetrameric hedgehog signaling complex. J. Biol. Chem. *275*, 21809–21812.

Sun, Z., Amsterdam, A., Pazour, G.J., Cole, D.G., Miller, M.S., and Hopkins, N. (2004). A genetic screen in zebrafish identifies cilia genes as a principal cause of cystic kidney. Development *131*, 4085–4093.

Taipale, J., Chen, J.K., Cooper, M.K., Wang, B., Mann, R.K., Milenkovic, L., Scott, M.P., and Beachy, P.A. (2000). Effects of oncogenic mutations in Smoothened and Patched can be reversed by cyclopamine. Nature *406*, 1005–1009.

Tay, S.Y., Ingham, P.W., and Roy, S. (2005). A homologue of the *Drosophila* kinesin-like protein Costal2 regulates Hedgehog signal transduction in the vertebrate embryo. Development *132*, 625–634.

Taylor, M.D., Liu, L., Raffel, C., Hui, C.C., Mainprize, T.G., Zhang, X., Agatep, R., Chiappa, S., Gao, L., Lowrance, A., et al. (2002). Mutations in SUFU predispose to medulloblastoma. Nat. Genet. *31*, 306–310.

Thor, S., Ericson, J., Brannstrom, T., and Edlund, T. (1991). The homeodomain LIM protein Isl-1 is expressed in subsets of neurons and endocrine cells in the adult rat. Neuron *7*, 881–889.

Todaro, G.J., and Green, H. (1963). Quantitative studies of the growth of mouse embryo cells in culture and their development into established lines. J. Cell Biol. *17*, 299–313.

Tsujikawa, M., and Malicki, J. (2004). Intraflagellar transport genes are essential for differentiation and survival of vertebrate sensory neurons. Neuron *42*, 703–716.

Varjosalo, M., Li, S.-P., and Taipale, J. (2006). Divergence of Hedgehog signal transduction mechanism between *Drosophila* and mammals. Dev. Cell *10*, this issue, 177–186.

Wang, G., Amanai, K., Wang, B., and Jiang, J. (2000). Interactions with Costal2 and suppressor of fused regulate nuclear translocation and activity of Cubitus interruptus. Genes Dev. *14*, 2893–2905.

Wolff, C., Roy, S., and Ingham, P.W. (2003). Multiple muscle cell identities induced by distinct levels and timing of hedgehog activity in the zebrafish embryo. Curr. Biol. *13*, 1169–1181.

Yamada, T., Pfaff, S.L., Edlund, T., and Jessell, T.M. (1993). Control of cell pattern in the neural tube: motor neuron induction by diffusible factors from notochord and floor plate. Cell *73*, 673–686.